ACS APPLIED MATERIALS & INTERFACES

Research Article

www.acsami.org

Collagen Gels with Different Fibrillar Microarchitectures Elicit Different Cellular Responses

Jing Xie,[†] Min Bao,[†] Stéphanie M. C. Bruekers, and Wilhelm T. S. Huck*

Institute for Molecules and Materials, Radboud University, Heyendaalseweg 135, 6525 AJ Nijmegen, The Netherlands

Supporting Information

ABSTRACT: The extracellular matrix consists of a complex mixture of fibrillar proteins, in which the architecture and mechanical properties of the protein fibrils vary considerably in various tissues. Here, we systematically polymerized collagen gels at different temperatures, providing substrates with tunable mechanics and defined local microarchitecture. We studied the dependence of spreading dynamics, proliferation, migration, and differentiation of human mesenchymal stem cells (hMSCs) on the fibrillar properties as compared to the bulk properties of the matrix. We found that high fiber stiffness, together with shorter fiber lengths, limited the transfer of cellular traction forces to nearby fibers. As a result, cells were not able to build up sufficient tension, which suppressed cell spreading, proliferation, and migration. Cells on such fibers also showed limited focal adhesion formation and different lineage selection preferences. In contrast, cell spreading, proliferation, and migration was always associated with fiber recruitment, long-range deformations in the collagen gel networks and an increase in collagen density around cells. Typically, cells on such substrates had a preference for osteogenic differentiation and showed higher levels of focal adhesions formation. These results contribute to a further understanding of the mechanotransduction process and to the design criteria for future biomimetic materials for tissue-engineering applications.

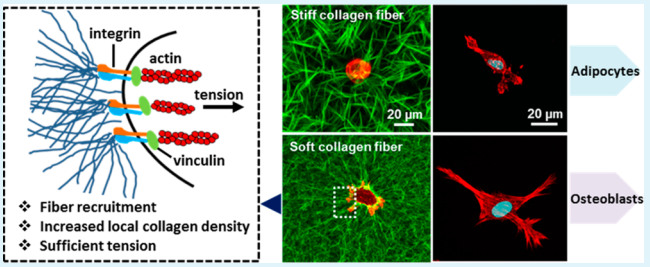

KEYWORDS: *collagen gels, fibrillar microenvironment, physical cues, fiber recruitment, force transmission*

1. INTRODUCTION

Cells can sense and transduce physical properties of the extracellular matrix (ECM) into intercellular signals that guide the cellular response.[1−6] Significant progress has been made in understanding these mechanosensing and mechanotransduction processes by studying cells on flat hydrogel substrates with tailored mechanical properties.[7−9] However, the native ECM is a complex and heterogeneous environment, making it very difficult to correlate specific materials properties of the ECM to cellular responses. Furthermore, as the ECM is composed of fibrous proteins (e.g., collagen, elastin, fibronectin, and laminin),[10,11] there is often a much-higher local stiffness (∼1 MPa at the individual-fiber level) compared to the bulk matrix (∼100 Pa at the bulk-matrix level).[12,13]

Baker et al.[14] recently designed a synthetic fibrous material with tunable mechanics and user-defined architecture that mimics key aspects of the fibrillar nature of the ECM. They found that lower fiber stiffness permitted cellular forces to recruit nearby fibers, thereby dynamically increasing ligand density at the cell surface and promoting the formation of focal adhesions (FAs) and related signaling. In contrast, networks of stiff fibers seemed to limit cell spreading. This is somewhat counterintuitive to the generally accepted notion that cells on softer surfaces often form fewer FAs and spread much less compared to stiff substrate. Baker et al. highlighted the importance of microstructure in synthetic fibrillar microenvironments. The aim of our work is to establish whether a similar mechanism holds true for matrices composed of fibrillar proteins instead of synthetic polymers to gain a deeper understanding of how local differences in structure and mechanics of the native ECM influence cell behavior.

Type I collagen is the predominant structural protein in the native ECM and forms fibrillar structure in various connective tissues, such as tendons, ligaments, and skin.[15−18] However, the structural and mechanical properties of collagen fibers vary depending upon their location in different tissues. For example, in areolar tissue, collagen fibers exhibit a loose arrangement and run in random directions. Compared to areolar tissue, the structure of tendons is completely different, as collagen fibers bunch up to form dense, rope-like bundles. In addition, collagen fibers localized in various tissues also differ greatly in mechanical properties, they are rigid in bone, compliant in skin, or form a gradient from rigid to compliant in cartilage.[19−22] A number of studies have reported detailed protocols to control the fiber thickness, stiffness, and length of collagen fibers, primarily by changing collagen concentration and polymerization temperature or pH.[17,23−30] Here, we expand these methods and study the response of hMSCs that are cultured on collagen gels composed of different fibers.

Received: March 20, 2017
Accepted: May 23, 2017
Published: May 24, 2017

DOI: 10.1021/acsami.7b03883
ACS Appl. Mater. Interfaces 2017, 9, 19630−19637

2. MATERIALS AND METHODS

2.1. Formation of Collagen Gels with Different Physical Cues. Fibrillar collagen gels were prepared from acid-solubilized rat-tail collagen I (BD Biosciences), as described previously.[26,31,32] Briefly, high-concentration collagen was diluted to 6 mg/mL with PBS, and then NaOH (1 N) was added to neutralize the pH; afterward, an equal amount of Dulbecco modified Eagle medium (DMEM)−Hepes (Gibco) was added to dilute the collagen to a 3 mg/mL solution. Finally, collagen gels with different physical cues were generated at different polymerization temperatures (4, 21, and 37 °C) and corresponding polymerization times of overnight (15 h), 2 h, and 30 min, respectively.

2.2. Mechanical Testing. We measured the bulk stiffness of collagen gels using an AR-G2 rheometer (TA Instruments, New Castle, DE). First, the polymerization temperature was set, and upon reaching the desired temperature, 700 μL of the gel solution was added to the 35 mm steel parallel plate with a 500 μm gap. Measurements were carried out at a controlled temperature of 4, 21, and 37 °C, respectively. After collagen had polymerized overnight (15 h) at 4 °C, 2 h at 21 °C, and 30 min at 37 °C, the shear storage modulus of the gels was measured at 1% strain at a frequency of 0.1 Hz for 30 min and all results were based on four separate experiments. Local fibers stiffness was measured by AFM (Bruker Nanoscope) using conical-tipped pyramidal cantilevers (NP-S type D, Bruker) at a 1 μm resolution, which was as close to the fiber diameter as possible. The "point-and-shoot" procedure (Nanoscope Software, Bruker) was used to measure fiber stiffness, and all of the gels were kept in PBS buffer during the measurement. To obtain fiber stiffness values from force curves, we used PUNIAS software (http://punias.free.fr). Specifically, multiple force displacement curves (five different locations) were fitted to the conical indenter Sneddon model:

$$F = \frac{2E \tan(\alpha)}{\pi(1 - \nu^2)}\delta^2$$

where F is the force, E is the Young's modulus, δ is the indentation depth, $\alpha = 18°$ is the indenter half-angle, and ν is the Poisson ratio, which was set to 0.5 on the indentation curve.[33]

2.3. Morphology of Collagen Microarchitecture. After collagen gel formation, immunostaining with a fluorescently labeled collagen antibody allowed us to observe the microarchitecture and the gel reorganization using confocal microscopy. Immunostaining was carried out by first staining with antibody antimouse collagen (Abcam, ab90395) for 1 h and subsequently by staining with secondary antibody Alexa-Fluor 488 goat anti-mouse (Thermo Fisher Scientific, R37120) for 1 h. During the experiment, all of the antibodies were dissolved in 1% BSA (Sigma). Finally, a Leica SP8 confocal laser scanning microscope (Leica, Germany) was used to take images and monitor the reorganization of the collagen fibers.

2.4. Quantification of Fibrillar Structure of Gels. We quantified the fibrillar structure of gels formed at 4 °C; due to extensive overlap of fibers in gels formed at higher temperatures, no accurate measurements could be performed. To calculate fiber diameter, length, and porosity, Alexa-Fluor 488-labeled collagen gels were imaged on an SP8 confocal microscope with a 63× objective. A total of 20 frames of Z-stacks were captured and merged into a single image by Image 5D Fiji software. From these images, an inverted threshold (dark threshold) was used to calculate the percent area that was not considered a fiber and used as a percent porosity measurement. For fiber diameter and length analysis, line segments were drawn across the widths and lengths of fibrils found in merged images for Col-4 using Fiji software. The number of independent experiments (N) was 3, and the number of data points (n) was ≥20; more than 20 regions of interest (ROI) from three separate experiments were analyzed.

2.5. hMSCs Culture and Seeding. hMSCs were obtained from Lonza and cultured to passage 6 in normal medium containing low-glucose DMEM, fetal bovine serum (FBS; Gibco), glutamine, and penicillin−streptomycin (pen/strep, Thermo Fisher Scientific). Next, hMSCs (P6) were seeded on the gels at the density of 1250 per cm^2 for cellular spreading, proliferation, migration, and microenvironment reorganization tests and 2500 or 25 000 per cm^2 for osteogenic and adipogenic differentiation, respectively. Proliferation medium (high-glucose DMEM + 10% FBS + 1% glutamine +1% pen/strep) was used to culture cells on different collagen gels except for differentiation studies; differentiation medium was composed of proliferation medium and osteogenic and adipogenic chemical supplements (5×10^{-7} M dexamethasone, 5 mM β-glycerolphosphate, 0.1 mM ascorbic acid-2-phosphate, 250 μM 3-isobutyl-1-methylxanthine, 5 μg/mL insulin, and 5×10^{-8} M rosiglitazone maleate, all from Sigma).

2.6. Time-Lapse Imaging. Nikon Diaphot 300 with Hamamatsu C8484−05G CCD Camera and a Leica SP8 confocal microscope were used to monitor cell movements and collagen fibers reorganization. During all experiments, cells were cultured at constant 37 °C and 7.5% CO_2 atmosphere, and microscopes were used to take images at 10 min intervals. For cell movements, we used a Nikon Diaphot 300 with a 10× phase contrast objective to track cells over 15 h. Next, the movement of single cell was measured by manually clicking on the geometric center of the cell using ImageJ Manual Tracking Plugin, and the xy coordinate corresponding to each clicked pixel was recorded. Trajectory graphs were generated by inputting the data into "Plot_At_Origin" program provided in a previous study.[34] For images of Alexa-Fluor 488-labeled collagen fibers reorganization, the 488 nm argon laser of a Leica SP8 confocal microscope was used, and all of the images were merged by Fiji software.

2.7. Immunofluorescence Staining. Immunofluorescent staining was performed to observe the cytoskeleton or FAs. After incubation, cells seeded on the gels were fixed with 4% paraformaldehyde (Sigma) for 10 min and treated in 0.2% Triton X-100 (Sigma) for 10 min at room temperature. For cytoskeleton staining, samples were incubated with phalloidin-Atto 633 (Sigma) and 4',6-diamidino-2-phenylindole (DAPI) (Millipore) for 1 h; for FAs staining, nonspecific binding sites were blocked in 10% BSA solution for 1 h first, followed by incubation with primary antibody antivinculin (Abcam, ab18058) and anti-integrin β1 antibody (ab30394) for 1 h and, subsequently, with secondary antibody Alexa 488 goat anti-mouse (Thermo Fisher Scientific, R37120), phalloidin, and DAPI for 1 h. The stained cells were imaged using the SP8, and spreading areas and perimeter measurements were obtained using Fiji's in-built "Measure" function after drawing a region of interest around cells. More than 80 cells were measured in three separate experiments.

2.8. Proliferation Test. For proliferation testing, EdU labeling, which can incorporate into the DNA of cells during replication, was performed. hMSCs were plated on different substrate at a density of 1250 per cm^2 and allowed to recover overnight, followed by treatment with 1× EdU solution. When the incubation up to 48 h, cells were fixed and permeabilized with 4% PFA and 0.1% Triton X-100, respectively. Following these processes, samples were treated according to the manufacturer's protocol of Click-iT EdU Alexa Fluor-488 HCS Assay (Thermo Fisher Scientific). All images were collected by a Leica SP8 confocal microscope (Leica, Germany) with filters for DAPI and Alexa Fluor-488. For quantification, lower magnification (10× objective) fields were collected within regions of interest.

2.9. Differentiation Assays. hMSCs were cultured for 7 or 10 days in mixture medium for osteogenic and adipogenic differentiation, respectively. Subsequently, all cells were fixed with 4% PFA and penetrated with 0.2% Triton-X 100 for 10 min, respectively. ALP staining was performed by Fast Blue assay (naphthol-AS-MSC phosphate and Fast Blue RR, Sigma) in Tris−HCl buffer (pH 8.9) and incubated at 37 °C for 1 h. Oil Red O staining was performed by incubating cells with 1.8 mg/mL Oil Red O (Sigma) for 30−60 min at room temperature and then rinsing with 60% isopropanol (Sigma). The nuclei were stained with DAPI, and images were acquired on a Zeiss inverted microscope (Photometrics, USA).

2.10. Statistics. Statistical analysis was performed with Origin software and one-way analysis of variance (ANOVA) using a Tukey post-test for more than two variables was carried out. "Significant" and "very significant" differences were indicated by * ($P < 0.05$) or ** ($P < 0.01$), respectively. All results were expressed as mean ± standard

DOI: 10.1021/acsami.7b03883
ACS Appl. Mater. Interfaces 2017, 9, 19630−19637

error. In each test, the number of independent experiments (N) is more than three, and the number of data points (n) in each experiment is different. Both N and n are shown in the figure legend.

3. RESULTS

3.1. Formation of Collagen Gels with Different Physical Properties. To investigate how cells sense local fibrillar microenvironments with different physical cues, we tuned the collagen gel microarchitecture by varying the polymerization temperature while maintaining the collagen concentration at 3 mg/mL, as previously reported.[26,32] This method gives us access to a number of well-controlled gel morphologies with different mechanical properties and local topography. We do note that changing the polymerization temperature leads to a change in physical parameters, including fiber stiffness and topography. As shown in Figure 1A–C,

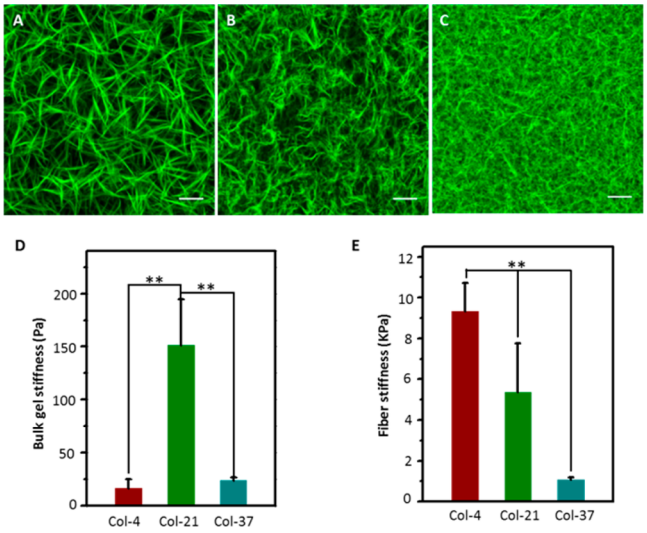

Figure 1. Collagen gels polymerized at different temperature with tunable mechanical and architectural features. (A–C) Morphologies of Alexa-Fluor 488-labeled collagen gels polymerized at 4, 21, and 37 °C, respectively. (D) Stiffness of bulk gels; $N = 4$. (E) Stiffness of local fibers; $N = 4$, $n = 5$. Scale bars: 20 μm. **: $P < 0.01$.

collagen fibers formed at higher temperature exhibited a more-compact structure and thinner fibers compared to those formed at lower temperature. Although we cannot accurately measure collagen fibers for gels polymerized at 21 and 37 °C (denoted as Col-21 and Col-37), fiber diameter and pore size appeared larger (1.7 ± 0.4 and 7 ± 2 μm, respectively), while the length of fibers appeared to be shorter (about 31 ± 4 μm) for gels polymerized at 4 °C (denoted as Col-4). Bulk stiffness all of these three collagen gels were very soft with stiffness ranging from 16.4 to 151.5 Pa (Figure 1D). However, the local fiber stiffness measured by AFM revealed that fiber stiffness was much higher and varied over a much wider range (from 1.1 to 9.3 kPa) by simply decreasing the polymerization temperature from 37 to 4 °C. (Figure 1E).

3.2. Microarchitecture Influence on Cell Spreading and Proliferation. hMSCs were seeded on different gels of varying architecture at low cell densities (1250 cells/cm^2) to observe single cell behavior. Representative confocal microscopy and time lapse microscopy images of cell spreading morphologies on Col-4, Col-21, and Col-37 at different time points within 24 h incubation are presented in Figure 2A and Supplementary Movies 1–3. The spreading of hMSCs on Col-21 and Col-37 started with the formation of small protrusions at 2 h after seeding. However, cells on Col-4 exhibited a round state and failed to spread until 5 h of culture time. Quantification of cell perimeter and spreading area on Col-21 and Col-37 (Figure 2B,C) showed a rapid increase after cell seeding, followed by a steady state around 15 h of incubation. On Col-4, cell spreading occurred at a later stage (around 5 h), and it took more time for cells to reach a steady state (around 24 h). At the steady state, cells on all gels adopted a similar spindle-like morphology, and cell perimeters were comparable (Figure 2B); however, the spreading area was significantly lower for cells cultured on Col-4 (Figure 2C). Cell proliferation over 48 h of culture was measured by EdU staining[35] and showed the same tendency with spreading area. Cell proliferation on Col-37 with soft fibers was 1.7-fold higher compared to Col-4 with stiff fibers (Figure 2D). These results suggest that the characteristics of the local microenvironment have an important effect on both cell spreading and proliferation.

3.3. Cell-Mediated Remodeling of Fibrillar Microenvironment and Positive Correlation with Cell Spreading. Fiber recruitment has been described as a mechanism by which cells probe and respond to mechanics in fibrillar matrices. We hypothesized that the different physical properties of collagen gels alter the ability of cells to remodel the surrounding matrix. Remodeling can be visualized by culturing hMSCs on fluorescently labeled collagen hydrogels.

Interestingly, we observed that the remodeling on Col-37 and Col-21 started at very early stages, around 5 h after seeding, and deformed networks and collagen fiber alignments between cells were clearly observed (Figure 3A). However, cells on Col-4 were immobile without any recruitment of fibers. A closer look at the interaction between cells and the surrounding matrix demonstrated that cells on Col-37 and Col-21 formed protrusions and pulled the surrounding fibers directionally along the protrusions into a bundled, aligned, and condensed matrix (Figure 3A). After hMSCs were cultured for 15 h on collagen gels, cells on all substrates were able to remodel their surrounding matrix. This remodeling process could be followed in time in our live cell imaging experiments (Movies S1–S3). Compared with cells on Col-37 and Col-21, less formation of long collagen lines between cells was observed on Col-4 (Figure 3B).

3.4. Recruitment of Collagen Fibers Promotion of β1 Integrins and Vinculin Expression through Myosin-Mediated Cellular Contractility. Immunostaining for activated β1 integrin (major integrin involved in collagen binding)[36,37] revealed that compared with cells on Col-4, higher levels of β1 integrin was found in cells cultured on Col-37 (Figure 4A). Vinculin is a focal adhesion-associated protein connecting integrins to actin filaments and whose recruitment to FAs can be induced by integrins. To assess the spatial distribution of FAs, cells were fluorescently stained for vinculin. On Col-37, FAs frequently occur as clusters along cell protrusions and are located primarily at the cell periphery. In contrast, no clear FAs were found on Col-4. Taken together, the compact structure of Col-37 provides more anchoring sites and effective mechanical feedback, which can promote cell spreading. In addition, to transmit forces, integrins, via vinculin, couple to actomyosin motors, which mediate cell contraction to mechanically pull on adhesion sites and promote cell spreading.[38,39] To test if a complete loss of contractility would result in different cell behavior, cells were treated with

DOI: 10.1021/acsami.7b03883
ACS Appl. Mater. Interfaces 2017, 9, 19630–19637

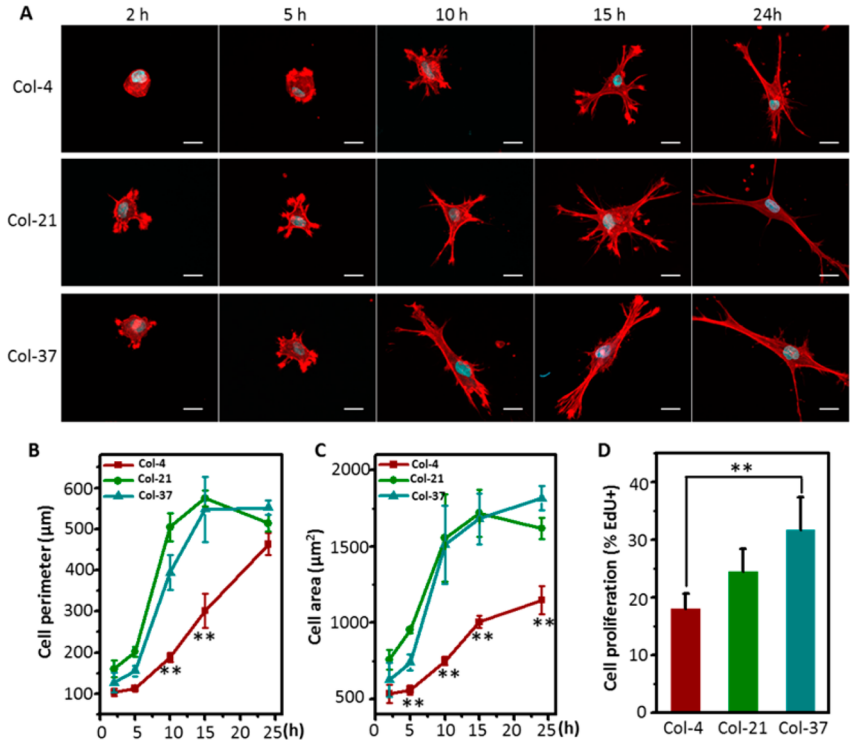

Figure 2. Cell spreading dynamics and proliferation. (A) Morphology of representative cells at different time points: cell skeleton staining with phalloidin (red) and nucleus staining with DAPI (blue). (B) Quantification of cell perimeter at different time points. (C) Quantification of cell area at different time points. (D) Proliferation of cells over 48 h as determined by EdU test. $N = 3$, $n \geq 80$. Scale bars: 20 μm. **: $P < 0.01$.

Blebbistatin (Bleb), an inhibitor of myosin II-mediated contractility but not adhesion to the collagen substrate.[40,41] Interestingly, significantly reduced fiber recruitment (Figure 5A) and local stiffness were observed after Bleb treatment (Figure 5B). These results confirm that local force generation, fiber recruitment, and strain stiffening by spreading cells depend upon β1 integrin−collagen interaction, focal adhesion assembly, and myosin II-mediated contractility.

3.5. Physical Cues of Fibrillar Microenvironment and Influence on hMSCs Migration. Previous studies have shown that there is a requirement for force in cell migration, and FAs are also known to be sensitive to force. Continuous force generation and effective feedback can promote not only FAs formation but cell migration. As shown in the time-lapse movies (Supplementary Movies 1−3), cells were inactive on Col-4 with delayed spreading and slow migration, during the whole culture time (15 h), the migration speed was only 0.14 μm/min. However, on Col-37 and Col-21, cells spread and migrated quickly, with 0.38 and 0.22 μm/min speed, respectively (Figure 6D). We tracked the migration of 25 representative cells on all gels (Figure 6A-C) and displayed all trajectories emanating from the origin. The movement of cells on Col-37 showed a substantially radial pattern; instead, on Col-4, cells stayed close to the initial position. In addition, according to the movement tracking and migration speed, cells on Col-37 showed significantly larger migration distances than the other two groups within the same time frame. All these migration quantitative analysis were performed according to the previous study.[42]

3.6. Fiber Recruitment Promotion of Osteogenic Differentiation of hMSCs. Finally stem cell fates were tested on different substrates. Osteogenic differentiation was determined by ALP staining, which is a marker for osteoblasts and the adipogenic differentiation, was detected using Oil Red O staining, specific for intracellular oil lipids. We found that under mixed medium conditions, hMSCs showed very significant differences in ALP and Oil Red O staining when differentiated on Col-37 and Col-4 (Figure 7 A). When hMSCs were cultured on Col-4, the ratio of osteogenic differentiation was 21.1%, much lower than that on Col-37 with 34.1% ALP positive (Figure 7 B). On the contrary, on Col-4 cells showed a preference for adipogenic differentiation, as up to 63.5% hMSCs were induced to adipocytes (Figure 7 C). These results indicate that the differentiation of hMSCs is related to physical properties of collagen fibers instead of bulk gels. Gels consisting of stiffer, shorter fibers appear to limit osteogenic differentiation and contribute to preferential differentiation to adipocytes.

4. DISCUSSION

While numerous studies have investigated the role of matrix stiffness in mediating cell behavior on both 2D and 3D substrates, much less is known about cell response to mechanics of ECM fibers.[43] In this study, we polymerized collagen at different temperature (4, 21, and 37 °C), leading to gels with varying physical properties, as previously shown.[31,44] In natural tissues, bulk stiffnesses range from several pascals (Pa) to many kilopascals (kPa), while the stiffness of the protein fibers of which these tissues are composed is often much higher, in the megapascal (MPa) range.[17] In our gels, we can engineer strongly different fiber stiffness while maintaining bulk stiffness below 200 Pa by changing the polymerization temperature without changing the density of collagen. As a result, we have a range of gel substrates that mimic some of the different fibrillar structures of the native ECM.

These structural and mechanical differences led us to investigate the effects of physical properties of fibrillar

DOI: 10.1021/acsami.7b03883
ACS Appl. Mater. Interfaces 2017, 9, 19630−19637

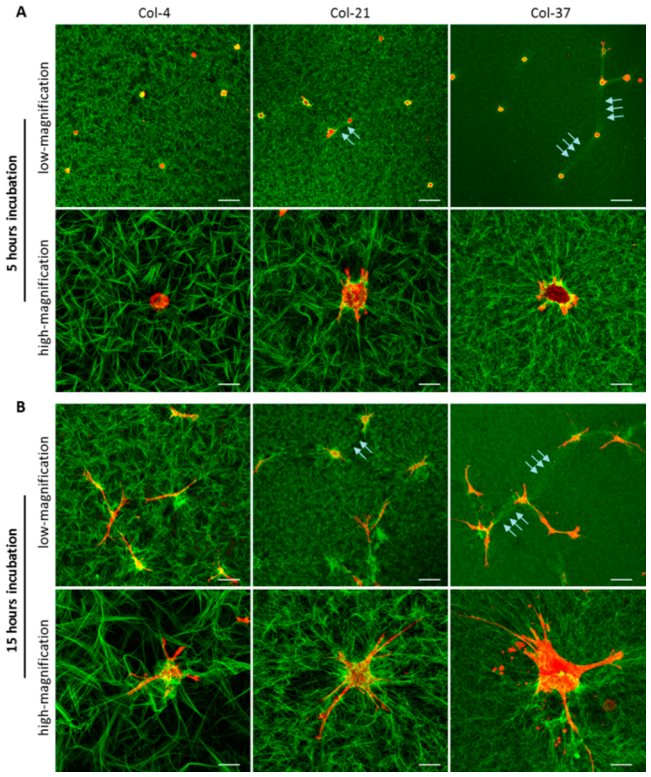

Figure 3. Mechanical remodeling of fibrillar microenvironment by hMSCs. (A) Cell-mediated initial recruitment after 5 h of incubation. (B) Collagen fibers became gradually disorganized after 15 h incubation. Actin cytoskeleton is stained with phalloidin (red), and collagen fiber is labeled with collagen antibody (green). Arrows indicate collagen lines formed between cells. Scale bars are 200 μm for images at low magnification (top) and 20 μm for images at high magnification (bottom).

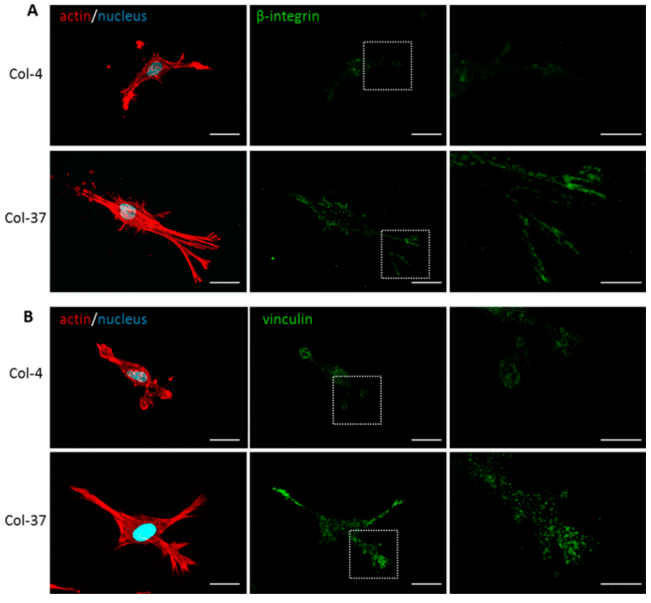

Figure 4. Mechanical remodeling of fibrillar microenvironment and promotion of β-integrin and FAs formation. (A) β-integrins and (B) FAs formation of representative hMSCs on Col-4 and Col-37 after 24 h of culturing. Merged images (left, scale bars: 20 μm). Single-channel images at low- and high-magnification overviews (middle, scale bars: 20 μm; right, scale bars: 100 μm).

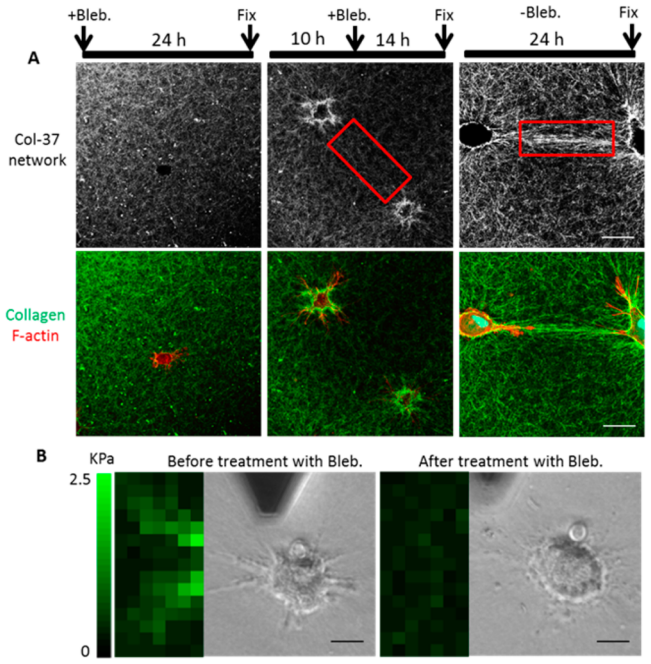

Figure 5. Myosin IIa-mediated cell contractility and induction of fiber recruitment. (A) Cell spreading after inhibition of Myosin IIa with Bleb treatment before (left images) or during (middle images) cell culture. Cells without Bleb treatment are the control (right images). Scale bars: 200 μm. (B) Local stiffness heat map of Col-37 before and after Bleb treatment. Heat maps were generated over the corresponding positions of bright-field images and represent the Young's modulus at each probing position. Scale bars: 20 μm.

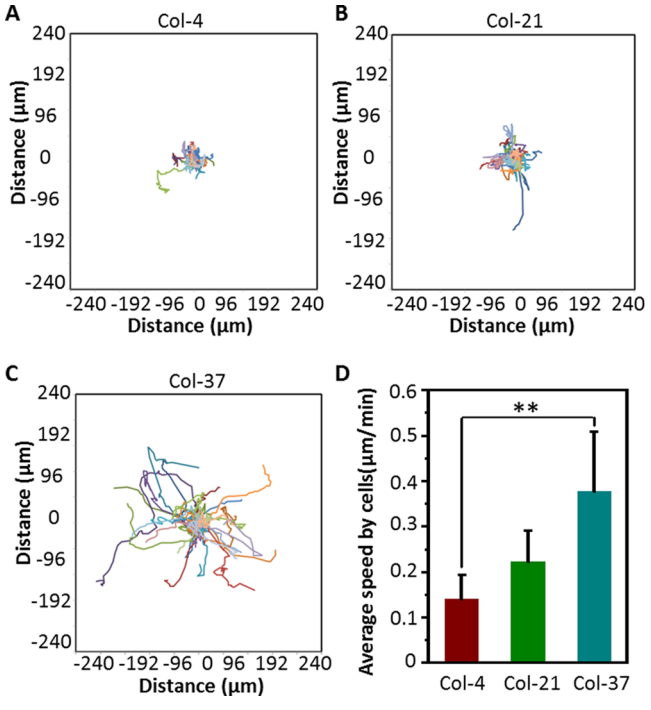

Figure 6. Cell migration influenced by fibrillar properties. (A–C) Movement tracking of 25 representative cells after 15 h of culturing on gels. (D) Average speed of cells on different collagen gels. **: $P < 0.01$; *: $P < 0.05$; $n = 25$.

microenvironment on cell behavior. hMSCs, an often-used cell type for mechanotransduction studies,[2,45,46] were seeded at a

DOI: 10.1021/acsami.7b03883
ACS Appl. Mater. Interfaces 2017, 9, 19630–19637

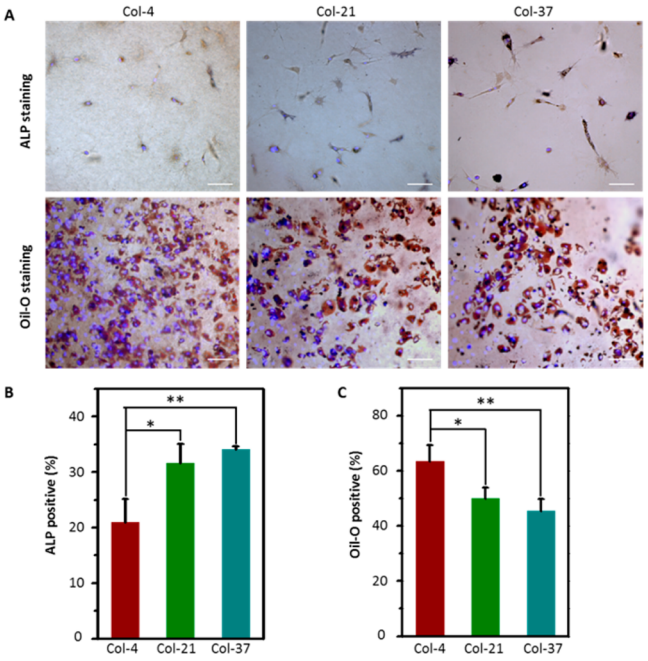

Figure 7. Cells differentiation dependence on substrate properties. (A) ALP and Oil-O staining showing osteogenic and adipogenic differentiation of hMSCs. (B) Quantitative results of positive osteogenic differentiation. (C) Quantitative results of positive adipogenic differentiation. Scale bars: 250 μm. **: $P < 0.01$; *: $P < 0.05$; $N = 3$; $n \geq 100$.

relatively low cell density to observe cellular responses (spreading, proliferation, migration, and differentiation) that are primarily determined by the local ECM differences, keeping the contribution of cell−cell interactions to a minimum. Several earlier studies on synthetic hydrogels surfaces have shown a strong correlation between hydrogel bulk stiffness and cell adhesion, spreading, proliferation and differentiation.[1,7,47,48] In contrast, we found that lower fiber stiffness permitted increased cell area, while stiff fibers suppressed cell spreading. Our results are consistent with Baker's recent study, where fibers made from polymer materials with lower-stiffness-enabled cells to remodel the surrounding matrix, leading to a larger spreading.[14] In addition, other research has shown that hMSC spreading, proliferation, and focal adhesion formation are dependent on ligand density but not on the fiber mechanics of hyaluronic acid hydrogels.[49] However, in that study, the fiber stiffness ranged from 1.1 to 8.6 GPa, which is too stiff for cells to recruit. In that case, cell behavior was indeed only regulated by ligand density.

We found that cell proliferation on Col-37 was 1.7-fold higher than on Col-4 with same the collagen density. On Col-37 gels, cells pulled and deformed the networks, resulting in significant recruitment of fibers to the cell and the formation of numerous densely compacted clusters of fibers, and this increased collagen density around cells and long-range force transmission appears to directly promote cell growth and spreading. Conversely, cells were unable to remodel the Col-4 gels, as the short, stiff fibers were unable to create long-range aligned structures upon cell traction (Figure S1), leading to negligible overall architectural remodeling, a low proliferation rate, and limited cell spreading.

These findings are in line with literature reports that have highlighted that the role of ECM fibers in long-range force transmission.[50−53] Despite these studies, little is known about the effect of fiber mechanics on force transmission. Our study has shown that soft fiber of collagen gel can facilitate long-range force transmission, while cells on stiff fibers could not because the fiber is too stiff and short. Due to limitations of fiber recruitment and force transmission, the population of β-integrin and FAs undergoing retraction at the leading edge were reduced. Via integrin-based adhesion sites, cells can mechanically sense physical surroundings and adjust mechanisms of migration[54,55] through the processes of protrusion, adhesion, translocation, and retraction. Thus, on Col-4, because of fewer FAs, the formation of leading edge protrusions was delayed. The strongly remodeled collagen bundles formed in Col-37 clearly do promote FAs formation and force transmission and guide cell migration along the bundles.

Numerous studies have demonstrated a strong correlation between hydrogel stiffness and cell differentiation, where stiff substrate promoted stem cells to differentiate into osteoblasts, while cells on soft substrate preferentially differentiated toward adipocytes.[1,2,56] However, in our study, we used soft gels with bulk stiffness below 200 Pa and found that more hMSCs differentiated toward osteoblasts on soft fibers (Col-37 gels).

5. CONCLUSIONS

In this study, we investigated how physical cues from the fibrillar microenvironment of collagen gels influence cell behavior. We formed collagen gels with different fibrillary architecture by polymerizing a constant concentration of 3 mg/mL collagen at different temperatures. We find that the ability of cells to remodel the gels is a major factor in determining whether cells can spread, proliferate, and migrate on these gels. Lower polymerization temperatures lead to shorter, thicker, and stiffer collagen fibers that appear less able to reorganize over larger length scales as the fibers lose connectivity upon reorganization by cells. As a result, cells show much-slower spreading when compared to gels with similar bulk stiffness but with longer, more-flexible fibers that can be easily remodeled. These differences in adhesion and spreading are also apparent in the much lower levels of focal adhesions on gels consisting of short and stiff fibers, and cells tend to differentiate toward adipocytes on these substrates. Our study highlights the importance of a better understanding of the role of fiber architecture of the natural ECM on cellular behavior.

■ ASSOCIATED CONTENT

Supporting Information

The Supporting Information is available free of charge on the ACS Publications website at DOI: 10.1021/acsami.7b03883.

A figure showing cell-mediated fiber recruitment of Col-4 and Col-37. (PDF)

Time-lapse video shows cell spreading and migration on Col-4 gel over 15 h. (AVI)

Time-lapse video shows cell spreading and migration on Col-21 gel over 15 h. (AVI)

Time-lapse video shows cell spreading and migration on Col-37 gel over 15 h. (AVI)

■ AUTHOR INFORMATION

Corresponding Author

*E-mail: w.huck@science.ru.nl.

ORCID

Min Bao: 0000-0003-0992-9388

Wilhelm T. S. Huck: 0000-0003-4222-5411

DOI: 10.1021/acsami.7b03883
ACS Appl. Mater. Interfaces 2017, 9, 19630−19637

Author Contributions

†J.X. and M.B. contributed equally.

Notes

The authors declare no competing financial interest.

■ ACKNOWLEDGMENTS

We acknowledge José M. A. Hendrik for assistance with cell cultures and Dr. Liesbeth Pierson for assistance with confocal microscopy. We are grateful to the China Scholarship Council and the Radboud Nanomedicine Alliance for financial support of this work.

■ REFERENCES

(1) Discher, D. E.; Janmey, P.; Wang, Y.-l. Tissue Cells Feel and Respond to the Stiffness of Their Substrate. *Science* **2005**, *310*, 1139−1143.
(2) Engler, A. J.; Sen, S.; Sweeney, H. L.; Discher, D. E. Matrix Elasticity Directs Stem Cell Lineage Specification. *Cell* **2006**, *126*, 677−689.
(3) Humphrey, J. D.; Dufresne, E. R.; Schwartz, M. A. Mechanotransduction and Extracellular Matrix Homeostasis. *Nat. Rev. Mol. Cell Biol.* **2014**, *15*, 802−812.
(4) Unadkat, H. V.; Hulsman, M.; Cornelissen, K.; Papenburg, B. J.; Truckenmüller, R. K.; Carpenter, A. E.; Wessling, M.; Post, G. F.; Uetz, M.; Reinders, M. J.; et al. An Algorithm-Based Topographical Biomaterials Library to Instruct Cell Fate. *Proc. Natl. Acad. Sci. U. S. A.* **2011**, *108*, 16565−16570.
(5) Trappmann, B.; Gautrot, J. E.; Connelly, J. T.; Strange, D. G.; Li, Y.; Oyen, M. L.; Cohen Stuart, M. A.; Boehm, H.; Li, B.; Vogel, V.; et al. Extracellular-Matrix Tethering Regulates Stem-Cell Fate. *Nat. Mater.* **2012**, *11*, 642−649.
(6) You, J.; Raghunathan, V. K.; Son, K. J.; Patel, D.; Haque, A.; Murphy, C. J.; Revzin, A. Impact of Nanotopography, Heparin Hydrogel Microstructures, and Encapsulated Fibroblasts on Phenotype of Primary Hepatocytes. *ACS Appl. Mater. Interfaces* **2015**, *7*, 12299−12308.
(7) Yeung, T.; Georges, P. C.; Flanagan, L. A.; Marg, B.; Ortiz, M.; Funaki, M.; Zahir, N.; Ming, W.; Weaver, V.; Janmey, P. A. Effects of Substrate Stiffness on Cell Morphology, Cytoskeletal Structure, and Adhesion. *Cell Motil. Cytoskeleton* **2005**, *60*, 24−34.
(8) Watt, F. M.; Huck, W. T. Role of the Extracellular Matrix in Regulating Stem Cell Fate. *Nat. Rev. Mol. Cell Biol.* **2013**, *14*, 467−473.
(9) Puklin-Faucher, E.; Sheetz, M. P. The Mechanical Integrin Cycle. *J. Cell Sci.* **2009**, *122*, 179−186.
(10) Hay, E. D. Extracellular Matrix. *J. Cell Biol.* **1981**, *91*, 205s−223s.
(11) Hynes, R. O. The Extracellular Matrix: Not Just Pretty Fibrils. *Science* **2009**, *326*, 1216−1219.
(12) Storm, C.; Pastore, J. J.; MacKintosh, F. C.; Lubensky, T. C.; Janmey, P. A. Nonlinear Elasticity in Biological Gels. *Nature* **2005**, *435*, 191−194.
(13) Collet, J.-P.; Shuman, H.; Ledger, R. E.; Lee, S.; Weisel, J. W. The Elasticity of an Individual Fibrin Fiber in a Clot. *Proc. Natl. Acad. Sci. U. S. A.* **2005**, *102*, 9133−9137.
(14) Baker, B. M.; Trappmann, B.; Wang, W. Y.; Sakar, M. S.; Kim, I. L.; Shenoy, V. B.; Burdick, J. A.; Chen, C. S. Cell-Mediated Fibre Recruitment Drives Extracellular Matrix Mechanosensing in Engineered Fibrillar Microenvironments. *Nat. Mater.* **2015**, *14*, 1262−1268.
(15) Badylak, S. F.; Freytes, D. O.; Gilbert, T. W. Extracellular Matrix as a Biological Scaffold Material: Structure and Function. *Acta Biomater.* **2009**, *5*, 1−13.
(16) Kadler, K. E.; Baldock, C.; Bella, J.; Boot-Handford, R. P. Collagens at a Glance. *J. Cell Sci.* **2007**, *120*, 1955−1958.
(17) Gautieri, A.; Vesentini, S.; Redaelli, A.; Buehler, M. J. Hierarchical Structure and Nanomechanics of Collagen Microfibrils from the Atomistic Scale Up. *Nano Lett.* **2011**, *11*, 757−766.
(18) Rother, S.; Salbach-Hirsch, J.; Moeller, S.; Seemann, T.; Schnabelrauch, M.; Hofbauer, L. C.; Hintze, V.; Scharnweber, D. Bioinspired Collagen/Glycosaminoglycan-Based Cellular Microenvironments for Tuning Osteoclastogenesis. *ACS Appl. Mater. Interfaces* **2015**, *7*, 23787−23797.
(19) Ushiki, T. Collagen Fibers, Reticular Fibers and Elastic Fibers. A Comprehensive Understanding from a Morphological Viewpoint. *Arch. Histol. Cytol.* **2002**, *65*, 109−126.
(20) Rho, J.-Y.; Kuhn-Spearing, L.; Zioupos, P. Mechanical Properties and the Hierarchical Structure of Bone. *Med. Eng. Phys.* **1998**, *20*, 92−102.
(21) Kato, Y. P.; Christiansen, D. L.; Hahn, R. A.; Shieh, S.-J.; Goldstein, J. D.; Silver, F. H. Mechanical Properties of Collagen Fibres: A Comparison of Reconstituted and Rat Tail Tendon Fibres. *Biomaterials* **1989**, *10*, 38−42.
(22) Silver, F. H.; Christiansen, D. L.; Snowhill, P. B.; Chen, Y. Role of Storage on Changes in the Mechanical Properties of Tendon and Self-Assembled Collagen Fibers. *Connect. Tissue Res.* **2000**, *41*, 155−164.
(23) Yang, Y.-l.; Leone, L. M.; Kaufman, L. J. Elastic Moduli of Collagen Gels Can Be Predicted from Two-Dimensional Confocal Microscopy. *Biophys. J.* **2009**, *97*, 2051−2060.
(24) Miron-Mendoza, M.; Seemann, J.; Grinnell, F. The Differential Regulation of Cell Motile Activity through Matrix Stiffness and Porosity in Three Dimensional Collagen Matrices. *Biomaterials* **2010**, *31*, 6425−6435.
(25) Carey, S. P.; Kraning-Rush, C. M.; Williams, R. M.; Reinhart-King, C. A. Biophysical Control of Invasive Tumor Cell Behavior by Extracellular Matrix Microarchitecture. *Biomaterials* **2012**, *33*, 4157−4165.
(26) Raub, C. B.; Suresh, V.; Krasieva, T.; Lyubovitsky, J.; Mih, J. D.; Putnam, A. J.; Tromberg, B. J.; George, S. C. Noninvasive Assessment of Collagen Gel Microstructure and Mechanics Using Multiphoton Microscopy. *Biophys. J.* **2007**, *92*, 2212−2222.
(27) Chrobak, K. M.; Potter, D. R.; Tien, J. Formation of Perfused, Functional Microvascular Tubes in Vitro. *Microvasc. Res.* **2006**, *71*, 185−196.
(28) Yang, Y.-l.; Motte, S.; Kaufman, L. J. Pore Size Variable Type I Collagen Gels and Their Interaction with Glioma Cells. *Biomaterials* **2010**, *31*, 5678−5688.
(29) Rosenblatt, J.; Devereux, B.; Wallace, D. Injectable Collagen as a Ph-Sensitive Hydrogel. *Biomaterials* **1994**, *15*, 985−995.
(30) Yamamura, N.; Sudo, R.; Ikeda, M.; Tanishita, K. Effects of the Mechanical Properties of Collagen Gel on the in Vitro Formation of Microvessel Networks by Endothelial Cells. *Tissue Eng.* **2007**, *13*, 1443−1453.
(31) Doyle, A. D.; Carvajal, N.; Jin, A.; Matsumoto, K.; Yamada, K. M. Local 3d Matrix Microenvironment Regulates Cell Migration through Spatiotemporal Dynamics of Contractility-Dependent Adhesions. *Nat. Commun.* **2015**, *6*, 8720.
(32) Wolf, K.; Te Lindert, M.; Krause, M.; Alexander, S.; Te Riet, J.; Willis, A. L.; Hoffman, R. M.; Figdor, C. G.; Weiss, S. J.; Friedl, P. Physical Limits of Cell Migration: Control by Ecm Space and Nuclear Deformation and Tuning by Proteolysis and Traction Force. *J. Cell Biol.* **2013**, *201*, 1069−1084.
(33) Petrie, R. J.; Gavara, N.; Chadwick, R. S.; Yamada, K. M. Nonpolarized Signaling Reveals Two Distinct Modes of 3d Cell Migration. *J. Cell Biol.* **2012**, *197*, 439−455.
(34) Gorelik, R.; Gautreau, A. Quantitative and Unbiased Analysis of Directional Persistence in Cell Migration. *Nat. Protoc.* **2014**, *9*, 1931−1943.
(35) Limsirichaikul, S.; Niimi, A.; Fawcett, H.; Lehmann, A.; Yamashita, S.; Ogi, T. A Rapid Non-Radioactive Technique for Measurement of Repair Synthesis in Primary Human Fibroblasts by Incorporation of Ethynyl Deoxyuridine (Edu). *Nucleic Acids Res.* **2008**, *37*, e31−e31.
(36) Takada, Y.; Ye, X.; Simon, S. The Integrins. *Genome Biol.* **2007**, *8*, 215.

DOI: 10.1021/acsami.7b03883
ACS Appl. Mater. Interfaces 2017, 9, 19630−19637

(37) Hynes, R. O. Integrins: Bidirectional, Allosteric Signaling Machines. *Cell* **2002**, *110*, 673−687.
(38) Wozniak, M. A.; Modzelewska, K.; Kwong, L.; Keely, P. J. Focal Adhesion Regulation of Cell Behavior. *Biochim. Biophys. Acta, Mol. Cell Res.* **2004**, *1692*, 103−119.
(39) Vicente-Manzanares, M.; Ma, X.; Adelstein, R. S.; Horwitz, A. R. Non-Muscle Myosin Ii Takes Centre Stage in Cell Adhesion and Migration. *Nat. Rev. Mol. Cell Biol.* **2009**, *10*, 778−790.
(40) Straight, A. F.; Cheung, A.; Limouze, J.; Chen, I.; Westwood, N. J.; Sellers, J. R.; Mitchison, T. J. Dissecting Temporal and Spatial Control of Cytokinesis with a Myosin Ii Inhibitor. *Science* **2003**, *299*, 1743−1747.
(41) Even-Ram, S.; Doyle, A. D.; Conti, M. A.; Matsumoto, K.; Adelstein, R. S.; Yamada, K. M. Myosin Iia Regulates Cell Motility and Actomyosin−Microtubule Crosstalk. *Nat. Cell Biol.* **2007**, *9*, 299−309.
(42) Foster, L. J.; de Hoog, C. L.; Mann, M. Unbiased Quantitative Proteomics of Lipid Rafts Reveals High Specificity for Signaling Factors. *Proc. Natl. Acad. Sci. U. S. A.* **2003**, *100*, 5813−5818.
(43) Kubow, K. E.; Conrad, S. K.; Horwitz, A. R. Matrix Microarchitecture and Myosin Ii Determine Adhesion in 3d Matrices. *Curr. Biol.* **2013**, *23*, 1607−1619.
(44) Rhee, S.; Grinnell, F. Fibroblast Mechanics in 3d Collagen Matrices. *Adv. Drug Delivery Rev.* **2007**, *59*, 1299−1305.
(45) Huebsch, N.; Arany, P. R.; Mao, A. S.; Shvartsman, D.; Ali, O. A.; Bencherif, S. A.; Rivera-Feliciano, J.; Mooney, D. J. Harnessing Traction-Mediated Manipulation of the Cell/Matrix Interface to Control Stem-Cell Fate. *Nat. Mater.* **2010**, *9*, 518−526.
(46) Khetan, S.; Guvendiren, M.; Legant, W. R.; Cohen, D. M.; Chen, C. S.; Burdick, J. A. Degradation-Mediated Cellular Traction Directs Stem Cell Fate in Covalently Crosslinked Three-Dimensional Hydrogels. *Nat. Mater.* **2013**, *12*, 458−465.
(47) Pelham, R. J.; Wang, Y.-l. Cell Locomotion and Focal Adhesions Are Regulated by Substrate Flexibility. *Proc. Natl. Acad. Sci. U. S. A.* **1997**, *94*, 13661−13665.
(48) Mih, J. D.; Marinkovic, A.; Liu, F.; Sharif, A. S.; Tschumperlin, D. J. Matrix Stiffness Reverses the Effect of Actomyosin Tension on Cell Proliferation. *J. Cell Sci.* **2012**, *125*, 5974−5983.
(49) Kim, I. L.; Khetan, S.; Baker, B. M.; Chen, C. S.; Burdick, J. A. Fibrous Hyaluronic Acid Hydrogels That Direct Msc Chondrogenesis through Mechanical and Adhesive Cues. *Biomaterials* **2013**, *34*, 5571−5580.
(50) Shi, Q.; Ghosh, R. P.; Engelke, H.; Rycroft, C. H.; Cassereau, L.; Sethian, J. A.; Weaver, V. M.; Liphardt, J. T. Rapid Disorganization of Mechanically Interacting Systems of Mammary Acini. *Proc. Natl. Acad. Sci. U. S. A.* **2014**, *111*, 658−663.
(51) Ma, X.; Schickel, M. E.; Stevenson, M. D.; Sarang-Sieminski, A. L.; Gooch, K. J.; Ghadiali, S. N.; Hart, R. T. Fibers in the Extracellular Matrix Enable Long-Range Stress Transmission between Cells. *Biophys. J.* **2013**, *104*, 1410−1418.
(52) Wang, H.; Abhilash, A.; Chen, C. S.; Wells, R. G.; Shenoy, V. B. Long-Range Force Transmission in Fibrous Matrices Enabled by Tension-Driven Alignment of Fibers. *Biophys. J.* **2014**, *107*, 2592−2603.
(53) Hall, M. S.; Alisafaei, F.; Ban, E.; Feng, X.; Hui, C.-Y.; Shenoy, V. B.; Wu, M. Fibrous Nonlinear Elasticity Enables Positive Mechanical Feedback between Cells and Ecms. *Proc. Natl. Acad. Sci. U. S. A.* **2016**, *113*, 14043−14048.
(54) Ridley, A. J.; Schwartz, M. A.; Burridge, K.; Firtel, R. A.; Ginsberg, M. H.; Borisy, G.; Parsons, J. T.; Horwitz, A. R. Cell Migration: Integrating Signals from Front to Back. *Science* **2003**, *302*, 1704−1709.
(55) Lauffenburger, D. A.; Horwitz, A. F. Cell Migration: A Physically Integrated Molecular Process. *Cell* **1996**, *84*, 359−369.
(56) Dupont, S.; Morsut, L.; Aragona, M.; Enzo, E.; Giulitti, S.; Cordenonsi, M.; Zanconato, F.; Le Digabel, J.; Forcato, M.; Bicciato, S.; et al. Role of Yap/Taz in Mechanotransduction. *Nature* **2011**, *474*, 179−183.

DOI: 10.1021/acsami.7b03883
ACS Appl. Mater. Interfaces 2017, 9, 19630−19637